Molecular Pharmacology Fast Forward. Published on September 18, 2015 as DOI: 10.1124/mol.115.101030
This article has not been copyedited and formatted. The final version may differ from this version.



# Pharmacological analysis and structure determination of 7-methylcyanopindolol-bound $\beta_1$-adrenergic receptor

Tomomi Sato, Jillian Baker, Tony Warne, Giles A. Brown, Andrew G.W. Leslie, Miles Congreve and Christopher G. Tate

MRC Laboratory of Molecular Biology, Cambridge Biomedical Campus, Francis Crick Avenue, Cambridge CB2 0QH, UK; TS, TW, AGWL, CGT

Heptares Therapeutics Ltd, Biopark, Broadwater Road, Welwyn Garden City, Hertfordshire AL7 3AX, UK; GAB, MC

School of Life Sciences, University of Nottingham, Medical School, Queen's Medical Centre, Nottingham NG7 2UH, UK; JB

KEK High Energy Accelerator Research Organization, Institute of Materials Structure Science, Structural Biology Research Center, 1-1 Oho, Tsukuba, Ibaraki 305-0801, Japan; TS

Molecular Pharmacology Fast Forward. Published on September 18, 2015 as DOI: 10.1124/mol.115.101030
This article has not been copyedited and formatted. The final version may differ from this version.



**Structure of 7-methylcyanopindolol-bound $\beta_1$AR**

**Corresponding author:**

**Christopher G. Tate**, MRC Laboratory of Molecular Biology, Cambridge Biomedical Campus, Francis Crick Avenue, Cambridge CB2 0QH, UK.

Telephone: +(44) 1223 267073

Email: cgt@mrc-lmb.cam.ac.uk

**Number of pages: 35**

**Number of Tables: 4**

**Number of Figures: 7**

**Number of References: 38**

**Number of words in Abstract: 229**

**Number of words in Introduction: 723**

**Number of words in Discussion: 1156**

Molecular Pharmacology Fast Forward. Published on September 18, 2015 as DOI: 10.1124/mol.115.101030
This article has not been copyedited and formatted. The final version may differ from this version.



**List of non-standard abbreviations:**

$\beta_1$AR: $\beta_1$-adrenergic receptor

$\beta_2$AR: $\beta_2$-adrenergic receptor

Carazolol: 1-(9*H*-carbazol-4-yloxy)-3-(propan-2-ylamino)propan-2-ol

CHO, Chinese hamster ovary

CGP12177, (-)-4-(3-*tert*-butylamino-2-hydroxypropoxy)- benzimidazol-2-one

CGP20712A, 2-hydroxy-5-(2-[{hydroxy-3-(4-[1-methyl-4-trifluoromethyl-2-imidazolyl]phenoxy)propyl}amino]ethoxy)benzamide

Cyanopindolol: (*RS*)-4-[3-(*tert*-butylamino)-2-hydroxypropoxy]-1*H*-indole-2-carbonitrile

CRE-SPAP, reporter gene containing 6 cAMP response elements (CRE) upstream of a secreted placental alkaline phosphatase (SPAP) reporter gene

IBMX, 1-methyl-3-(2-methylpropyl)-7H-purine-2,6-dione

ICI 118551 (-)-1-(2,3-[dihydro-7-methyl-1H-inden-4-yl]oxy)-3-([1-methylethyl]-amino)-2-butanol

7-methylcyanopindolol, 4-[(2*S*)-3-(*tert*-butylamino)-2-hydroxypropoxy]-7-methyl-1*H*-indole-2-carbonitrile

T4L: T4 lysozyme

TM: transmembrane region

Molecular Pharmacology Fast Forward. Published on September 18, 2015 as DOI: 10.1124/mol.115.101030
This article has not been copyedited and formatted. The final version may differ from this version.



## Abstract

Comparisons between structures of the $\beta_1$-adrenergic receptor ($\beta_1$AR) bound to either agonists, partial agonists or weak partial agonists led to the proposal that rotamer changes of $Ser^{5.46}$, coupled to a contraction of the binding pocket, are sufficient to increase the probability of receptor activation. Cyanopindolol is a weak partial agonist of $\beta_1$AR and, based on the hypothesis above, we predicted that the addition of a methyl group to form 7-methylcyanopindolol would reduce dramatically its efficacy. An eight-step synthesis of 7-methylcyanopindolol was developed and its pharmacology analysed. 7-Methylcyanopindolol bound with similar affinity to cyanopindolol to both $\beta_1$AR and $\beta_2$AR. As predicted, the efficacy of 7-methylcyanopindolol was reduced significantly compared to cyanopindolol, acting as a very weak partial agonist of turkey $\beta_1$AR and an inverse agonist of human $\beta_2$AR. The structure of 7-methylcyanopindolol-bound $\beta_1$AR was determined to 2.4 Å resolution and found to be virtually identical to the structure of cyanopindolol-bound $\beta_1$AR. The major differences in the orthosteric binding pocket are that it has expanded by 0.3 Å in 7-methylcyanopoindol-bound $\beta_1$AR and the hydroxyl group of $Ser^{5.46}$ is positioned 0.8 Å further from the ligand with respect to the position of the $Ser^{5.46}$ side chain in cyanopindolol-bound $\beta_1$AR. Thus the molecular basis for the reduction in efficacy of 7-methylcyanopindolol compared to cyanopindolol may be regarded as the opposite of the mechanism proposed for the increase in efficacy of agonists compared to antagonists.

Molecular Pharmacology Fast Forward. Published on September 18, 2015 as DOI: 10.1124/mol.115.101030
This article has not been copyedited and formatted. The final version may differ from this version.



## Introduction

The $\beta_1$ and $\beta_2$ adrenergic receptors ($\beta_1$AR and $\beta_2$AR) are well-studied prototypical members of the G protein-coupled receptor (GPCR) superfamily (Venkatakrishnan et al., 2013). *In vivo*, the receptors are activated by both adrenaline and noradrenaline, with important clinical roles in modulation of cardiac output ($\beta_1$AR) and bronchodilatation ($\beta_2$AR). Recent successes in the structure determination of both $\beta_1$AR (Warne et al., 2008; Moukhametzianov et al., 2011; Warne et al., 2011; Warne et al., 2012; Christopher et al., 2013; Miller-Gallacher et al., 2014) and $\beta_2$AR (Cherezov et al., 2007; Wacker et al., 2010; Rosenbaum et al., 2011; Rasmussen et al., 2011a; Rasmussen et al., 2011b) have led to a molecular understanding of receptor activation (Lebon et al., 2012). Binding of a full agonist to the receptors results in a contraction of the ligand binding pocket by 1.0 Å for $\beta_1$AR and 1.2 Å for $\beta_2$AR and a rotamer change of $Ser^{5.46}$ so that it forms a hydrogen bond with the *para*-hydroxyl group of the catecholamine moiety of the agonist. However, the agonist-bound receptors remain in an overall conformation that is consistent with an inactive state. The role of the agonist is thus to increase the probability of active state formation, but the agonist is insufficient on its own to stabilize the active state. A crystal structure of $\beta_2$AR in the active state bound to the heterotrimeric G protein Gs (Rasmussen et al., 2011b) showed that the fully active state is characterized by the formation of a cleft in the intracellular face of the receptor and a 16 Å outward movement of the cytoplasmic end of transmembrane helix 6 (H6).

Structures have been determined of $\beta_1$AR bound to full agonists (Warne et al., 2011), partial agonists (Warne et al., 2011), weak partial agonists (Warne et al., 2008; Moukhametzianov et al., 2011; Miller-Gallacher et al., 2014) and biased agonists (Warne et al., 2012). All these structures are in an inactive state, so the structures with

agonists represent the encounter complex between the ligand and receptor before the receptor becomes activated. As mentioned above, full agonists cause a contraction of the binding pocket and cause a rotamer change of $Ser^{5.46}$ due to hydrogen bond formation. In addition, there is a rotamer change of $Ser^{5.42}$. The combination of these changes results in the weakening of helix-helix interactions between H3, H4 and H5 that has been proposed to be the important initial event that increases the probability of the receptor adopting an active conformation (Warne and Tate, 2013). In support of this, partial agonists cause a contraction of the binding pocket, the rotamer change of $Ser^{5.42}$, but not the rotamer change of $Ser^{5.46}$. Weak partial agonists cause only the rotamer change of $Ser^{5.42}$, but not of $Ser^{5.46}$ and they do not cause the contraction of the ligand binding pocket due to the additional oxymethylene spacer in the backbone of the ligand (Fig 1). Thus there appears to be a direct correlation between specific differences in the structure of the receptor-ligand complex and the efficacy of the ligand.

A prediction of the molecular mechanism for agonist activation of $\beta_1$AR is that the efficacy of a ligand should be reduced upon the addition of a methyl group in the position analogous to the *para*-hydroxyl of, for example, isoprenaline (Warne et al., 2011), to prevent the rotamer change of $Ser^{5.46}$ by steric hindrance (see Fig. 1 for structures of ligands discussed in the text). To test this hypothesis, we therefore made the methylated version of cyanopindolol, 7-methylcyanopindolol. Cyanopindolol was used as the starting point for this study because its properties are pharmacologically and structurally well defined. Through the single modification of cyanopindolol to make 7-methylcyanopindolol, we could be certain that the only effect would be on the rotamer comformation of $Ser^{5.46}$. In this way we could be certain that any changes in efficacy were due to this modification and not any other differences in the ligand.

Molecular Pharmacology Fast Forward. Published on September 18, 2015 as DOI: 10.1124/mol.115.101030
This article has not been copyedited and formatted. The final version may differ from this version.



## Materials and methods

**Materials.** 7-Methylcyanopindolol (4-[(2*S*)-3-(*tert*-butylamino)-2-hydroxypropoxy]-7-methyl-1*H*-indole-2-carbonitrile) was synthesized as described below. $^{3}$H-CGP12177, $^{3}$H-adenine and $^{14}$C-cAMP were from Amersham International (Buckinghamshire, UK) and Microscint 20 and Ultima Gold XR scintillation fluid were from PerkinElmer (Shelton, CT, USA). Foetal calf serum was from PAA Laboratories (Teddington, Middlesex, UK). CGP20712A was from Tocris Life Sciences (Avonmouth, UK). S-Cyanopindolol, carazolol, ICI 118551, isoprenaline and propranolol were from Sigma Chemicals (Poole, Dorset, UK). DM (n-decyl-β-D-maltopyranoside) was purchased from Anatrace (Maumee, USA). Monoolein was from Nu Chek Prep (Elysian, USA). CHS (cholesteryl hemisuccinate) and cholesterol were purchased from Sigma-Aldrich (Dorset, England).

## Cell culture

Pharmacological studies were conducted in CHO cells stably expressing either the turkey $\beta_1$AR (CHO-tβ1, receptor expression level 148 fmol/mg protein, defined as tβtrunc in (Baker, 2010b) or the human $\beta_2$-adrenoceptor (CHO-hβ2, receptor expression level 466 fmol/mg protein; (Baker et al., 2003)). Both of these cell lines also contained the stably transfected reporter gene CRE-SPAP. Negative control cells were parental CHO cells (CHO-CRE-SPAP cells), which are CHO cells with the stably transfected reporter but without any transfected receptor (Baker et al., 2003). Cells were grown in Dulbecco's modified Eagle's medium nutrient mix F12 (DMEM/F12) containing 10% foetal calf serum and 2 mM L-glutamine in a 37°C humidified 5% $CO_2$ : 95% air atmosphere.

Molecular Pharmacology Fast Forward. Published on September 18, 2015 as DOI: 10.1124/mol.115.101030
This article has not been copyedited and formatted. The final version may differ from this version.



**$^{3}$H-CGP12177 whole cell binding**

Ligand affinity was measured using $^{3}$H-CGP12177 whole cell binding as previously described (Baker, 2010a). Briefly, cells were grown to confluence in white-sided, clear-bottomed 96-well view plates. The following day, the media was removed and replaced with 100 μl of serum-free media containing the competing ligand at twice the final required concentration followed immediately by 100 μl of $^{3}$H-CGP12177. After 2 hours incubation (37°C, 5% $CO_2$), the cells were washed twice by the addition and removal of 200 μl phosphate buffered saline (4ºC). A white base was applied to the plate, 100 μl Microscint 20 was added to each well, a sealant top applied to the top of the plate, and after at least 8 hours at room temperature, the plates were counted on a TopCount (PerkinElmer) at 21°C for 2 minutes per well. Propranolol (10 μM final concentration) was used to determine non-specific binding in all cases. All data points were performed in triplicate and each 96-well plate also contained 6 determinations of total and non-specific binding.

**$^{3}$H-cAMP accumulation**

Cells were grown to confluence in 24-well plates. The following day, the cells were pre-labelled with $^{3}$H-adenine (2 hours incubation with 0.5 ml media containing 1 μCi $^{3}$H-adenine). The $^{3}$H-adenine was removed, the cells washed by the addition and removal of 1 ml serum-free media, then 1 ml serum-free media containing 1 mM IBMX was added to each well. After 15 minutes, 10 μl ligand was added to each well and incubated for 5 hours (37°C, 5% $CO_2$). The reaction was terminated by the addition of 50 μl concentrated HCl per well, the plates frozen and thawed and $^{3}$H-cAMP separated from other $^{3}$H-nucleotides by sequential Dowex and alumina column

Molecular Pharmacology Fast Forward. Published on September 18, 2015 as DOI: 10.1124/mol.115.101030
This article has not been copyedited and formatted. The final version may differ from this version.



chromatography, as previously described (Baker, 2010b). Basal activity and a positive control (response to 10 μM isoprenaline) were included in all plates for every experiment. Responses are therefore expressed as a percentage of this maximum, or in the case of inverse agonists, as a percentage of the basal response.

**Data analysis**

For whole cell binding, a sigmoidal binding curve (equation 1) was fitted to the concentration response curves using Graphpad Prism 2.01 and the $IC_{50}$ was then determined as the concentration required to inhibit 50% of the specific binding.

Equation 1: $$\% \text{ uninhibited binding} = 100 - \frac{(100 \times A)}{(A + IC_{50})} + NS$$

A is the concentration of the competing ligand, $IC_{50}$ is the concentration at which half of the specific binding of $^3$H-CGP12177 has been inhibited, and NS is the non-specific binding.

From this $IC_{50}$ value and the known concentration of $^3$H-CGP12177, a $K_D$ value (concentration at which half the receptors are bound by the competing ligand) was calculated using equation 2. The $K_D$ values for $^3$H-CGP12177 were 0.42 nM at the turkey $\beta_1$AR (Baker, 2010b) and 0.17 nM at the human $\beta_2$AR (Baker, 2010a).

Equation 2: $$K_D = \frac{IC_{50}}{1 + ([^3\text{H-CGP12177}]/K_D \text{ of } ^3\text{H-CGP12177})}$$

For functional responses ($^3$H-cAMP accumulation and CRE-SPAP gene transcription), most agonist responses were described by a one-site sigmoidal concentration response curve (equation 3):

Molecular Pharmacology Fast Forward. Published on September 18, 2015 as DOI: 10.1124/mol.115.101030
This article has not been copyedited and formatted. The final version may differ from this version.



Equation 3: $$\text{Response} = \frac{\text{Emax} \times [A]}{EC_{50} + [A]}$$

Emax is the maximum agonist response, [A] is the agonist concentration and $EC_{50}$ is the concentration of agonist that produces 50% of the maximal response

However, several of the responses were best described by a two-site concentration response (equation 4):

Equation 4: $$\%\ \text{maximal stimulation} = \frac{[A] \times N}{([A] + EC1_{50})} + \frac{[A] \times (100\text{-}N)}{([A] + EC2_{50})}$$

N is the percentage of site 1, [A] is the concentration of agonist and $EC1_{50}$ and $EC2_{50}$ are the respective $EC_{50}$ values for the two agonist sites.

All data are presented as the mean ± standard error of the mean (SEM) of n separate experiments.

**Synthesis of 4-[(2*S*)-3-(*tert*-butylamino)-2-hydroxypropoxy]-7-methyl-1*H*-indole-2-carbonitrile (7-MeCyp)**. The synthesis of 7-MeCyp was performed in an 8-step procedure (Fig. 2) that is described in detail below (Steps 1-8). Where no preparative routes are included, the relevant intermediate is commercially available. Commercial reagents were utilized without further purification. Room temperature (rt) refers to approximately 20-27°C. $^1$H NMR spectra were recorded at 400 MHz on either a Bruker or Jeol instrument. Chemical shift values are expressed in parts per million (ppm), *i.e.* (δ)-values. The following abbreviations are used for the multiplicity of the NMR signals: s = singlet, br = broad, d = doublet, t = triplet, m = multiplet. Coupling constants are listed as *J* values, measured in Hz. NMR and mass spectroscopy results were corrected to account for background peaks. Chromatography refers to column chromatography performed using 60-120 mesh silica gel and executed under nitrogen

pressure (flash chromatography) conditions. TLC for monitoring reactions refers to TLC run using the specified mobile phase and the Silica gel F254 as a stationary phase from Merck.

LCMS experiments were typically carried out using electrospray conditions as specified for each compound under the following conditions:

**Method A.** Instrument: Waters Acquity H-class UPLC with SQ detector using BEH C18 (50*2.1 mm id 1.7 μm) and using water (0.1% ammonium hydroxide) and MeCN (0.1% ammonium hydroxide) as the mobile phase. The eluent gradient program was MeCN (0.1% ammonium hydroxide) from 10% to 100% for 2.5 min, 100% MeCN (0.1% ammonium hydroxide) for 2 min and MeCN (0.1% ammonium hydroxide) from 100% to 10% for 0.5 min. The flow rate was 0.3 ml/min.

**Method B.** Instruments: HP1100 with HP DAD G1315A detector and Micromass ZQ using a Phenomenex Gemini-NX C-18, 3 micron, 2.0 x 30 mm column using water (0.1% ammonium hydroxide) and MeCN (0.1% ammonium hydroxide) as the mobile phase. The eluent gradient program was MeCN (0.1% ammonium hydroxide) from 0% to 95% for 8.4 min, 95% MeCN (0.1% ammonium hydroxide) for 1 min and MeCN (0.1% ammonium hydroxide) from 100% to 10% for 0.5 min. The flow rate was 1.5 ml/min, injection volume was 3 μl, column temperature 45 ˚C and UV detection from 230 nM to 400 nM.

**Step 1: Synthesis of 2-(benzyloxy)-5-methylbenzaldehyde.** 2-Hydroxy-5-methylbenzaldehyde (5.00 g, 36 mmol) was dissolved in DMF (30 ml), $K_2CO_3$ (6.07 g, 44 mmol) and benzyl bromide (4.36 ml, 36 mmol) were added, the reaction mixture was warmed to 65°C and stirred for 6 h. The reaction mixture was cooled to room temperature and poured into water (500 ml). The precipitate was filtered, washed with water (100 ml) and dried to give 2-(benzyloxy)-5-methylbenzaldehyde (7.0 g, 84 %

Molecular Pharmacology Fast Forward. Published on September 18, 2015 as DOI: 10.1124/mol.115.101030
This article has not been copyedited and formatted. The final version may differ from this version.



yield) as a white solid. **LCMS (Method A)**: m/z 227 $[M+H]^+$ ($ES^+$), at 3.14 min, 99.6%. **$^1$H NMR:** (400 MHz, DMSO-$d_6$) δ: 2.28 (s, 3H), 5.27 (s, 2H), 7.23 (d, $J$ = 8.5, 1H), 7.33 - 7.36 (m, 1H), 7.39 - 7.42 (m, 2H), 7.43 - 7.47 (m, 1H), 7.48 - 7.51 (m, 3H), 10.41 (br. s, 1H).

**Step 2: Synthesis of methyl 4-(benzyloxy)-7-methyl-1*H*-indole-2-carboxylate.** A solution of 2-(benzyloxy)-5-methylbenzaldehyde (1.87 g, 8.26 mmol) and methyl azidoacetate (4 ml, 40.8 mmol) in methanol (20 ml) was added drop wise to a solution of sodium metal (0.75 g, 33.04 mmol) in methanol (5 ml) at -20°C. The mixture was stirred at -8°C for 3 h and then poured onto ice, filtered and the precipitate was dissolved in xylene (20 ml). The reaction mixture was heated at 130°C for 18 h. The reaction mixture was then cooled to 0°C and the resulting precipitate was filtered and dried to give methyl 4-(benzyloxy)-7-methyl-1H-indole-2-carboxylate (0.9 g, 36 % yield) as a white solid. **LCMS (Method A)**: m/z 296 $[M+H]^+$ ($ES^+$), at 3.47 min, 100%. **$^1$H NMR:** (400 MHz, DMSO-$d_6$) δ: 2.43 (s, 3H), 3.87 (s, 3H), 5.21 (s, 2H), 6.55 (d, $J$ = 7.5, 1H), 6.94 (d, $J$ = 7.5, 1H), 7.17 - 7.18 (m, 1H), 7.32 - 7.35 (m,1H), 7.41 (t, $J$ = 7.5, 2H), 7.50 - 7.52 (m, 2H), 11.81 (br. s, 1H).

**Step 3: synthesis of 4-(benzyloxy)-7-methyl-1*H*-indole-2-carboxylic acid.** Methyl 4-(benzyloxy)-7-methyl-1H-indole-2-carboxylate (0.9 g, 3.0 mmol) was dissolved in ethanol (30 ml) and 2N NaOH was added (41.4 ml, 105 mmol), the reaction mixture was stirred for 4 h at 90°C. The reaction mixture was cooled to room temperature and acidified to pH 4 with aqueous 3N HCl. The precipitate was filtered, wash with water (100 ml) and dried to give 4-(benzyloxy)-7-methyl-1H-indole-2-carboxylic acid (0.7 g, 82% yield) as a white solid. **LCMS (Method A)**: m/z 280 $[M-H]^+$ ($ES^-$), at 3.16 min, 100%. **$^1$H NMR:** (400 MHz, DMSO-$d_6$) δ: 2.41 (s, 3H), 5.19 (s, 2H), 6.49 (d, $J$ = 7.5, 1H), 6.84 (d, $J$ = 7.5, 1H), 6.97 (s, 1H), 7.31 - 7.34 (m, 1H),

7.40 (t, *J* = 7.5, 2H), 7.49 - 7.51 (m, 2H), 11.27 (br. s, 1H), one exchangeable proton not observed.

**Step 4: synthesis of 4-(benzyloxy)-7-methyl-1*H*-indole-2-carboxamide.** 4-(benzyloxy)-7-methyl-1H-indole-2-carboxylic acid (0.9 g, 3.1 mmol) was dissolved in diethyl ether (18 ml). Thionyl chloride (0.78 g, 6.5 mmol) was added at 0°C and the reaction mixture stirred at room temperature for 5 h. The solvents were removed *in vacuo* and the residues were dissolved in diethyl ether (10 mL). The reaction mixture was cooled to -20°C and ammonia gas was bubbled through for 5 min. The solvents were removed *in vacuo* and the crude product was purified by column chromatography (normal phase silica, 10 to 20% ethyl acetate in hexane) to give 4-(benzyloxy)-7-methyl-1H-indole-2-carboxamide (0.6 g, 67% yield) as a white solid. **LCMS (Method A)**: m/z 281 $[M+H]^+$ ($ES^+$), at 3.04 min, 99.4%. **$^1$H NMR:** (400 MHz, DMSO-$d_6$) δ: 2.42 (s, 3H), 5.18 (s, 2H), 6.52 (d, *J* = 7.5, 1H), 6.85 (d, *J* = 7.5, 1H), 7.25 - 7.27 (m, 2H), 7.32 - 7.35 (m, 1H), 7.42 (t, *J* = 7.5, 2H), 7.50 - 7.52 (m, 2H), 7.91 (br. s, 1H), 11.34 (br. s, 1H).

**Step 5: synthesis of 4-hydroxy-7-methyl-1*H*-indole-2-carboxamide.** 4-(Benzyloxy)-7-methyl-1H-indole-2-carboxamide (0.6 g, 2.4 mmol) was dissolved in methanol (20 ml) and 10% Pd/C (0.2 g, 1.8 mmol) was added. The reaction mixture was stirred at room temperature under 1 atm of $H_2$ gas for 8 h. The reaction mixture was filter through celite and the solvents were removed *in vacuo* to give 4-hydroxy-7-methyl-1H-indole-2-carboxamide (0.4 g, 86% yield) as a white solid. **LCMS (Method A)**: m/z 191 $[M+H]^+$ ($ES^+$), at 0.59 min, 80.5%. **$^1$H NMR:** (400 MHz, DMSO-$d_6$) δ: 2.37 (s, 3H), 6.28 (d, *J* = 7.5, 1H), 6.73 (d, *J* = 7.5, 1H), 7.15 - 7.17 (m, 1H), 7.27 (br. s, 1H), 7.87 (br. s, 1H), 9.38 (br. s, 1H), 11.09 (br. s, 1H).

**Step 6: synthesis of 4-hydroxy-7-methyl-1*H*-indole-2-carbonitrile**. 4-Hydroxy-7-methyl-1H-indole-2-carboxamide (0.4 g, 2.1 mmol) was dissolved in 1,4-dioxane (4 ml). $POCl_3$ (0.5 ml) was added and the reaction mixture was stirred at 75°C for 15 min. The reaction mixture was cooled to room temperature partitioned and quenched with ammonia solution (5 mL), partitioned between $H_2O$ (50 ml) and EtOAc (100 ml), the aqueous layer was further extracted with EtOAc (3 x 100 ml), the organic layers were combined and dried ($Na_2SO_4$). Solvent was removed *in vacuo* the crude product was purified by column chromatography (normal phase silica, 15 to 20% ethyl acetate in hexane) to give 4-hydroxy-7-methyl-1H-indole-2-carbonitrile (0.2 g, 55% yield) as a yellow solid. **LCMS (Method A)**: m/z 171 $[M-H]^+$ ($ES^-$), at 1.56 min, 92.1%. **$^1$H NMR:** (400 MHz, DMSO-$d_6$) δ: 2.34 (s, 3H), 6.37 (d, $J$ = 7.5, 1H), 6.90 (d, $J$ = 7.5, 1H), 7.32 - 7.33 (m, 1H), 9.71 (br. s, 1H), 12.11 (br. s, 1H).

**Step 7: synthesis of 7-methyl-4-[(2*S*)-oxiran-2-ylmethoxy]-1*H*-indole-2-carbonitrile.** 4-Hydroxy-7-methyl-1H-indole-2-carbonitrile (0.25 g, 1.4 mmol) was dissolved in water (2.5 ml) and 1,4-dioxane (1 ml). NaOH (0.058 g, 1.4 mmol) was added followed by (S)-epichlorohydrine (1.25 ml, 0.58 mmol). The reaction mixture was stirred at room temperature for 16 h. The reaction mixture was partitioned between $H_2O$ (50 ml) and ethyl acetate (50 ml), the aqueous layer was further extracted with ethyl acetate (2 x 50 ml), the organic layers were combined and dried ($Na_2SO_4$). Solvent was removed *in vacuo* to give 7-methyl-4-[(2*S*)-oxiran-2-ylmethoxy]-1*H*-indole-2-carbonitrile (0.2 g, 60% yield) as a yellow gum which was used in the next step without further purification. **LCMS (Method A)**: m/z 229 $[M+H]^+$ ($ES^+$), at 1.94 min, 70%.

**Step 8: synthesis of 4-[(2*S*)-3-(*tert*-butylamino)-2-hydroxypropoxy]-7-methyl-1*H*-indole-2-carbonitrile.** 7-methyl-4-[(2*S*)-oxiran-2-ylmethoxy]-1*H*-indole-

Molecular Pharmacology Fast Forward. Published on September 18, 2015 as DOI: 10.1124/mol.115.101030
This article has not been copyedited and formatted. The final version may differ from this version.



2-carbonitrile (0.19 g, 0.8 mmol) was dissolved in tert-butylamine (2.85 ml, 26.9 mmol) and the reaction mixture was stirred at 70°C for 8 h. The solvent was removed *in vacuo* and the residue was purified by reverse phase prep HPLC [X Bridge, C-18, 150×30 mm, 5 μm, 30 ml per min, gradient 50% to 100% (over 10 min) then 100% (2 min) acetonitrile in 10% acetonitrile/water)] to give 4-[(2*S*)-3-(*tert*-butylamino)-2-hydroxypropoxy]-7-methyl-1*H*-indole-2-carbonitrile (0.02 g, 8% yield) as a light yellow solid. **LCMS (Method B)**: m/z 302 $[M+H]^+$ ($ES^+$), at 3.95 min, 100%. **$^1$H NMR:** (400 MHz, DMSO-$d_6$) δ: 1.09 (s, 9H), 2.36 (s, 3H), 2.56 – 2.68 (m, 2H), 3.83 – 3.86 (m, 1H), 3.93 – 3.97 (m, 1H), 4.02 – 4.06 (m, 1H), 6.48 (d, *J* = 7.8, 1H), 6.99 (d, *J* = 7.8, 1H), 7.30 (s, 1H), 12.26 (br. s, 1H). Two exchangeable protons were not observed. **$^{13}$C NMR:** (400 MHz, DMSO-$d_6$) δ: 16.45, 29.25, 45.63, 50.17, 69.38, 71.22, 101.62, 104.73, 111.47, 114.42, 115.24, 117.72, 126.70, 138.40, 151.32.

**Expression, purification, and crystallization of $\beta_1$AR.** The β44-TS construct was used, which contained additional thermostabilising mutations, I129$^{3.40}$V, E130$^{3.41}$W, Y343$^{7.53}$L (Miller and Tate, 2011) to the previously published turkey (*Meleagris gallopavo*) $\beta_1$AR construct, β44-m23 (Warne et al., 2009; Warne et al., 2011). The construct used here is identical to that used for the structure determination of $\beta_1$AR at 2.1 Å resolution (Miller-Gallacher et al., 2014), except that it contains the E130$^{3.41}$W mutation to improve the amount of functional receptor expressed and Asp322 is identical to the wild type receptor, instead of being mutated to Lys to form a salt bridge in the extracellular region. None of these mutations affect the structure of the binding pocket of the receptor. Ballesteros-Weinstein numbers are shown as superscripts (Ballesteros, 1995).

Expression of β44-TS using recombinant baculovirus and receptor purification were all performed as described previously (Warne et al., 2003; Warne et al., 2009), although expression was performed in High Five™ cells grown in ESF921 medium (Expression systems). A 2-fold increase in functional expression to 8 mg/L culture was observed with this construct compared with β44-m23, which is most likely attributable to the inclusion of the mutation E130$^{3.41}$W (Roth et al., 2008). Solubilisation of the receptor from the membrane fraction was performed using 1.5% DM and all buffers used in the purification contained 0.1% DM. Purified receptor was competitively eluted from the final alprenolol Sepharose affinity column with 100 μM 7-methyl-cyanopindolol in buffer [20 mM Tris-HCl (pH 7.6), 0.35 M NaCl, 0.1% DM and 1 mM EDTA (pH 8.0)]. For desalting and concentration, the sample (15 – 20 ml) was concentrated to 0.1 ml using an Amicon-ultra concentrator (Ultracel-50K; Millipore), diluted 5 – 10-fold in dilution buffer [20 mM Tris-HCl (pH 7.6), 0.1 M NaCl, 0.1% DM, 0.1 mM EDTA and 1 mM 7-methyl-cyanopindolol] and concentrated down again to 0.1 ml. This step was repeated twice and finally receptor was concentrated to 30 – 50 mg/ml. Before crystallization, CHS was added from a concentrated stock (10 mg/ml in 2% DM) to give a final concentration of 2 mg/ml CHS and 0.4% DM. Protein determination was performed using the amido black assay (Schaffner and Weissmann, 1973).

Crystals were generated using the lipidic cubic phase (LCP) method in monoolein. Monoolein and purified receptor were drawn into two separate Hamilton syringes in a 3:2 (v:v) ratio of monoolein:protein solution. 100 nl of the protein:lipid mixture was dispensed on a plastic plate, overlaid by 500 nl of precipitant solution (18 – 36% PEG 600 and 0.1 M ADA pH 7.0) in each well with a mosquito-LCP (TTP Labtech), sealed with a plastic cover, and stored in a humidified 23˚C incubator.

Molecular Pharmacology Fast Forward. Published on September 18, 2015 as DOI: 10.1124/mol.115.101030
This article has not been copyedited and formatted. The final version may differ from this version.



Crystals grew as thin plates in LCP and reached maximum dimensions of 200 × 200 x ~10 μM. Crystals were directly picked from LCP and cryo-cooled in liquid nitrogen.

**Data collection, structure solution and refinement**

Diffraction data were collected from 4 cryo-cooled crystals on beamline ID29 (wavelength, 0.9723Å) at the European Synchrotron Radiation Facility (Grenoble, France) and on beamline I24 (wavelength, 0.9687Å) at the Diamond Light Source (Oxfordshire, UK). Thirteen wedges of data from 4 crystals were merged. Images were processed with MOSFLM (Leslie, 2006) and AIMLESS (Evans, 2006; Evans, 2011). The structure was solved by molecular replacement with PHASER (McCoy et al., 2007) using the $\beta_1$AR-LCP structure with cyanopindolol bound (Miller-Gallacher et al., 2014) as a starting model. Refinement, rebuilding and validation were carried out with REFMAC5 (Murshudov et al., 1997; Murshudov et al., 2011), COOT (Emsley et al., 2010) and MOLPROBITY (Davis et al., 2007; Chen et al., 2010).

**Results**

**The affinity of 7-methylcyanopindolol for turkey $\beta_1$AR and human $\beta_2$AR**

7-Methylcyanopindolol was synthesized in an 8-step process to yield 20 mg of pure product as defined by LCMS and the structure was confirmed by $^{1}$H and $^{13}$C NMR (see Methods). The affinity of 7-methylcyanopindolol for turkey $\beta_1$AR and human $\beta_2$AR was compared with other well-characterized antagonists through competition binding assays using $^{3}$H-CGP12177 and performed on whole cells (Fig. 3 and Table I). The affinity of turkey $\beta_1$AR for 7-methylcyanopindolol was 43 ± 3 pM (n=6), which is very similar to its affinity for cyanopindolol (35 ± 3 pM, n=6). Human $\beta_2$AR

Molecular Pharmacology Fast Forward. Published on September 18, 2015 as DOI: 10.1124/mol.115.101030
This article has not been copyedited and formatted. The final version may differ from this version.



bound both ligands with similar affinities to turkey $\beta_1$AR. The affinities of the receptors for two other antagonists (used in the efficacy studies below), carazolol and ICI118551, were also determined and were found to be similar to previous determinations (Baker, 2010a; Baker, 2010b).

**The efficacy of 7-methylcyanopindolol at turkey $\beta_1$AR**

Previous studies have shown a large response window in $^3$H-cAMP accumulation measurements in a CHO cell line stably expressing turkey $\beta_1$AR (CHO-t$\beta_1$, 148 fmol of receptor per mg protein) to measure small responses in ligand efficacy (Baker, 2010a). Isoprenaline stimulated an increase in $^3$H-cAMP accumulation that was 22.5 ± 1.3 fold over basal, confirming a large response window (n=4; Fig. 4). As previously observed (Baker, 2010b), cyanopindolol elicited a biphasic response curve with the maximum response reaching 31.8 ± 1.1% (n=4) of the response elicited by the full agonist isoprenaline (Table II). In contrast, 7-methylcyanopindolol gave a response that reached a maximum of 2.3 ± 0.3% (n=4) of that attained by isoprenaline. Whilst it appeared that this response was best described by a single site sigmoidal response curve, a second component cannot be excluded because the increase in $^3$H-cAMP was so small. ICI118551, a potent inverse agonist of $\beta_2$AR (Bond et al., 1995; Azzi et al., 2001), gave no response. Carazolol was previously described as a partial inverse agonist of the human $\beta_2$AR (Rosenbaum et al., 2007) although other studies have shown it to stimulate a partial agonist response at the human $\beta_1$AR and $\beta_2$AR (Baker, 2010a) and the turkey $\beta_1$AR . Here, carazolol was again shown to be a weak partial agonist of turkey $\beta_1$AR, and it elicited a biphasic response similar to that seen for cyanopindolol (Fig. 4 and Table II), and similar to that seen at the human $\beta_1$AR (Baker, 2010a).

Molecular Pharmacology Fast Forward. Published on September 18, 2015 as DOI: 10.1124/mol.115.101030
This article has not been copyedited and formatted. The final version may differ from this version.



**The efficacy of 7-methylcyanopindolol at human $\beta_2$AR**

The results from the previous section indicated that 7-methylcyanopindolol was an exceedingly weak partial agonist of turkey $\beta_1$AR, but as no convincing inverse agonism was detected in this assay with ICI118551, the experiments were repeated on human $\beta_2$AR (cell line CHO-hβ2, receptor expression level 466 fmol receptor per mg protein), which has higher basal activity than $\beta_1$AR (Engelhardt et al., 2001). Isoprenaline stimulated a large increase in $^3$H-cAMP accumulation in CHO-β2 cells (61.4 ± 5.4 (n=8) fold over basal; Fig. 4). Cyanopindolol was found to stimulate an agonist response (with a maximum stimulation of 8.0 % that of isoprenaline, Figure 4, Table III) and a small stimulation was also seen in response to carazolol. When 7-methyl-cyanopindolol was examined, there was no increase in $^3$H-cAMP accumulation, but rather a very small decrease in basal activity. As inverse agonism has previously been reported in this cell line (Baker et al., 2003), the response to 7-methylcyanopindolol was examined alongside that of the known inverse agonist ICI118551 (Fig. 4). ICI118551 was confirmed to have inverse agonist activity resulting in a decrease of basal activity by 55%. The inverse activity of 7-methyl-cyanopindolol was found to be less, causing a decrease in basal activity by 25%.

**Efficacy of 7-methylcyanopindolol in CRE-gene transcription responses**

The β-antagonist propranolol acts as an inverse agonist of the G protein-coupled pathway, causing a decrease in cAMP production, but it stimulates CRE-gene transcription in the CHO-hβ2 cell line through signaling via the G protein-independent MAP kinase pathway through β-arrestins (Baker et al., 2003). As 7-methylcyanopindolol was found to be a weak inverse agonist, its response at the level

of CRE-gene transcription was also investigated. For turkey $\beta_1$AR, the CRE-gene transcription responses observed for cyanopindolol was similar to the response in the $^3$H-cAMP accumulation studies (Fig. 5, Table II), but no response was detected for 7-methylcyanopindolol. For human $\beta_2$AR, an agonist response was observed for cyanopindolol, but 7-methylcyanopindolol did not stimulate an increase in CRE-SPAP production (Figure 5, Table III). There is thus no evidence for biased signaling through β-arrestins by 7-methylcyanopindolol.

Negative control experiments in CHO-CRE-SPAP cells (*i.e.* with no transfected receptor) showed that 10 μM forskolin stimulated a response that was 18.3 ± 4.7 fold over basal (n=4) in the $^3$H-cAMP accumulation assay (not shown) and 5.9 ± 0.5 fold over basal (n=4) in the CRE-gene transcription assays. No response was observed in CHO-CRE-SPAP cells upon addition of either cyanopindolol, 7-methyl-cyanopindolol, carazolol or isoprenaline (n=4 in each case; Figure 5).

**Structure of 7-methylcyanopindolol-bound $\beta_1$AR**

To produce high-quality crystals of $\beta_1$AR, a thermostabilized version of the receptor was used that contained 9 thermostabilizing mutations in addition to truncations at the N-terminus, C-terminus and cytoplasmic loop 3 (see Materials and Methods). Thermostabilized $\beta_1$AR was expressed using the baculovirus expression system, purified by $Ni^{2+}$-affinity chromatography and alprenolol sepharose affinity chromatography (Warne et al., 2003; Warne et al., 2009) and crystallized using the lipidic cubic phase technique (Miller-Gallacher et al., 2014). Data were collected at synchrotron microfocus beamlines and the structure determined by molecular replacement and refined to a final resolution of 2.4 Å (Table IV). The final model contained one receptor molecule per asymmetric unit, associated with 2 $Na^+$ ions, 5

lipids and 28 water molecules, with good density for 7-methylcyanopindolol in the ligand binding pocket (Fig. 6). The receptor is in the inactive state and is virtually identical to the structure of cyanopindolol-bound receptor (PDB code 4BVN; RMSD 0.19 Å over 2062 atoms) (Miller-Gallacher et al., 2014). The major difference in the ligand binding pocket between $\beta_1$AR bound to either cyanopindolol or 7-methylcyanopindolol is that the hydroxyl group of Ser215$^{5.46}$ is displaced 0.8 Å from its position when cyanopindolol is bound, in a direction away from the center of the receptor.

## Discussion

The synthesis of 7-methylcyanopindolol has allowed further understanding of the components that affect ligand efficacy in $\beta_1$AR. Previous data suggested that the rotamer change of Ser215$^{5.46}$ and a contraction of the ligand binding pocket were sufficient to increase the probability of formation of the activated state of the receptor (Warne et al., 2011; Warne and Tate, 2013). Therefore ligands that prevented rotamer changes of Ser215$^{5.46}$ and prevented contraction of the orthosteric binding pocket should, in theory, have greatly reduced efficacy and may even become inverse agonists. Cyanopindolol was described previously as a weak partial agonist of both human and turkey $\beta_1$AR (Baker, 2010a; Baker, 2010b) and so we therefore synthesized 7-methylcyanopindolol, with the methyl group in a position predicted to dramatically decrease its efficacy. Pharmacological analysis of 7-methylcyanopindolol showed that it bound with similar high affinity to both turkey $\beta_1$AR and human $\beta_2$AR, and that there was a marked reduction in efficacy at both receptors. However, at the turkey $\beta_1$AR, 7-methylcyanopindol was an exceedingly weak partial agonist whereas for $\beta_2$AR the ligand acted as a weak partial inverse

agonist. Thus the goal was achieved in reducing efficacy, but raised the question of why a tiny amount of agonist activity could still be detected at $\beta_1$AR, whereas ICI118551 did not elicit any response.

In efforts to further understand the molecular mechanism of 7-methylcyanopindolol, the structure of 7-methylcyanopindolol-bound $\beta_1$AR was determined at 2.4 Å resolution, which is sufficient to determine unambiguously the rotamer conformation and precise positioning of serine side chains. Comparison of this structure with structures of $\beta_1$AR bound either to cyanopindolol (Miller-Gallacher et al., 2014) or carazolol (Moukhametzianov et al., 2011), both weak partial agonists, showed that the binding pocket was actually slightly larger than expected by 0.3-0.5 Å, as measured between the Cα atoms of Ser211$^{5.42}$ and Asn329$^{7.39}$. In addition, there was a difference in position of the hydroxyl group of Ser215$^{5.46}$ in the 7-methylcyanopindolol-bound structure compared to the cyanopindolol-bound structure of 0.8 Å, in a direction away from the ligand, presumably due to the proximity of the methyl group of 7-methyl cyanopindolol. Both the increase in size of the binding pocket and the outward shift of the hydroxyl group of Ser215$^{5.46}$ are consistent with the dramatic reduction in efficacy of 7-methylcyanopindolol compared to cyanopindolol. If an analogous comparison is performed in the structures of $\beta_2$AR bound to the weak partial agonist carazolol (Cherezov et al., 2007) and the inverse agonist ICI118551 (Wacker et al., 2010), exactly the same differences are observed, *i.e.* an expansion of the binding pocket of 0.4 Å (measured as above) and a 0.7 Å shift of the hydroxyl group of Ser207$^{5.46}$ (Fig. 7).

Although Ser215$^{5.46}$ appears to be a major determinant in defining ligand efficacy, two other serine residues have also been implicated by mutagenesis in the activation of β-receptors, namely Ser211$^{5.42}$ and Ser212$^{5.43}$ (Strader et al., 1989;

Liapakis et al., 2000). The orientation of Ser211$^{5.42}$ has been suggested to correlate with decreased efficacy of ligands, based on the comparison of $\beta_1$AR structures bound to 8 different ligands (Warne and Tate, 2013). Structures of $\beta_1$AR bound to agonists and partial agonists, including $\beta_1$AR bound to cyanopindolol and 7-methylcyanopindol, invariably have the side chain of Ser211$^{5.42}$ in a gauche$^+$ rotamer, whereas $\beta_1$AR bound to carazolol and carvedilol have Ser211$^{5.42}$ in a trans rotamer (see Fig. 7A). Thus one possibility to explain the residual agonist activity of 7-methylcyanopindolol is that the slight destabilization of the H5 interface between H3 and H4 caused by the gauche$^+$ orientation of the Ser211$^{5.42}$ side chain is sufficient to make the ligand an extremely weak partial agonist. The role of Ser212$^{5.43}$ in determining ligand efficacy is less clear, as it does not make direct contact to the ligand, but instead forms a hydrogen bond with Asn310$^{6.55}$ that may assist in orienting the side chain for optimal hydrogen bond formation with full agonists (Warne et al., 2011). As Asn310$^{6.55}$ forms van der Waals contacts with the weak partial agonists studied here, as opposed to a hydrogen bond with full agonists, then its effect may be minimal in determining the efficacy of the weak partial agonists given that different rotamers of Asn310$^{6.55}$ would presumably always be in weak van der Waals contact with the ligand. This view is supported by the absence of the Ser212$^{5.43}$-Asn310$^{6.55}$ hydrogen bond in one structure of cyanopindolol-bound $\beta_1$AR (Miller-Gallacher et al., 2014), although it is clearly present in other cyanopindolol-bound structures (Warne et al., 2008).

In considering the factors that dictate the efficacy of a ligand for $\beta_1$AR, there appears to be a hierarchy of factors that have a diminishing effect as you go down the list. Firstly, the most important factor is probably the contraction of the binding pocket upon agonist binding, which has been observed in all structures bound to full

or partial agonists (Warne et al., 2011). Without this contraction, it is unlikely that hydrogen bonds would be able to form between the catecholamine moiety of the agonist and the side chains of Ser215$^{5.46}$ and Ser211$^{5.42}$. Secondly, the rotamer change of Ser215$^{5.46}$ is important as this dictates the difference in binding between a full and partial agonist, and allows hydrogen bond formation to the ligand (Warne et al., 2011). Thirdly, the rotamer change of Ser211$^{5.42}$, in addition to its defining role in the binding of partial agonists, may promote lower levels of activity in antagonists when the binding pocket is less likely to contract and Ser215$^{5.46}$ is less likely to rotate due to steric clashes with the ligand (Warne and Tate, 2013). Currently, we do not know where in this hierarchy the importance of Ser212$^{5.43}$ falls. Mutagenesis suggests that this is an important residue in determining agonist affinity in $\beta_2$AR (Strader et al., 1989) and in the structures of $\beta_1$AR it usually forms a hydrogen bond with Asn310, that in turn forms a strong hydrogen bond to the catecholamine headgroup (or equivalent) when agonists bind to the receptor (Warne et al., 2011). As it appears that the hydrogen bond is present in the activated state of the $\beta_2$AR bound to the G protein mimic Nb80 (Rasmussen et al., 2011a), it seems likely that ligands which reduce the probability of this bond forming will have poor efficacy, although no such ligands have been described so far.

In conclusion, we have demonstrated that a single modification of cyanopindolol to make 7-methylcyanopindolol was sufficient to reduce dramatically the efficacy of the ligand and the structure of the ligand-receptor complex has confirmed the importance of the rotamer conformation of Ser215$^{5.46}$ in receptor activation and inverse agonist activity. The unexpected residual agonist activity of the ligand highlights the role of Ser211$^{5.42}$ in ligand-induced activation of $\beta_1$AR and that it

Molecular Pharmacology Fast Forward. Published on September 18, 2015 as DOI: 10.1124/mol.115.101030
This article has not been copyedited and formatted. The final version may differ from this version.



is not just playing a passive role in increasing ligand affinity. Further work will therefore be needed to finally make a high-affinity inverse agonist for $\beta_1$AR.

Coordinates and structure factors for 7-methylcyanopindolol-bound $\beta_1$AR have been deposited with the Protein Data Bank, PDB ID 5A8E.

**Acknowledgements**

Diffraction data were collected at the European Synchotron Radiation Facility, Grenoble (ID29) and at Diamond Light Source, Harwell (I24), we would like to thank beamline staff there for their continued assistance.

Molecular Pharmacology Fast Forward. Published on September 18, 2015 as DOI: 10.1124/mol.115.101030
This article has not been copyedited and formatted. The final version may differ from this version.



Authorship contributions

*Participated in Research design:* Sato, Baker, Warne and Tate

*Conducted experiments:* Sato, Baker, Brown and Warne

*Performed data analysis:* Sato, Baker, Warne and Leslie

*Wrote or contributed to the writing of the manuscript:* Sato, Baker, Brown, Warne, Congreve, Leslie and Tate

## References

Azzi M, Pineyro G, Pontier S, Parent S, Ansanay H, and Bouvier M (2001) Allosteric effects of G protein overexpression on the binding of beta-adrenergic ligands with distinct inverse efficacies. *Mol Pharmacol* **60**: 999-1007.

Baker JG (2010a) The selectivity of beta-adrenoceptor agonists at human beta1-, beta2- and beta3-adrenoceptors. *Br J Pharmacol* **160**: 1048-1061.

Baker JG (2010b) A full pharmacological analysis of the three turkey beta-adrenoceptors and comparison with the human beta-adrenoceptors. *PLoS One* **5**: e15487.

Baker JG, Hall IP, and Hill SJ (2003) Agonist and inverse agonist actions of beta-blockers at the human beta 2-adrenoceptor provide evidence for agonist-directed signaling. *Mol Pharmacol* **64**: 1357-1369.

Ballesteros JAW, H (1995) Integrated methods for the construction of three dimensional models and computational probing of structure function relations in G protein-coupled receptors. *Methods Neurosci* **25**: 366–428

Bond RA, Leff P, Johnson TD, Milano CA, Rockman HA, McMinn TR, Apparsundaram S, Hyek MF, Kenakin TP, Allen LF, and et al. (1995) Physiological effects of inverse agonists in transgenic mice with myocardial overexpression of the beta 2-adrenoceptor. *Nature* **374**: 272-276.

Chen VB, Arendall WB, 3rd, Headd JJ, Keedy DA, Immormino RM, Kapral GJ, Murray LW, Richardson JS, and Richardson DC (2010) MolProbity: all-atom structure validation for macromolecular crystallography. *Acta Crystallogr D Biol Crystallogr* **66**: 12-21.

Cherezov V, Rosenbaum DM, Hanson MA, Rasmussen SG, Thian FS, Kobilka TS, Choi HJ, Kuhn P, Weis WI, Kobilka BK, and Stevens RC (2007) High-resolution crystal structure of an engineered human beta2-adrenergic G protein-coupled receptor. *Science* **318**: 1258-1265.

Christopher JA, Brown J, Dore AS, Errey JC, Koglin M, Marshall FH, Myszka DG, Rich RL, Tate CG, Tehan B, Warne T, and Congreve M (2013) Biophysical fragment screening of the beta1-adrenergic receptor: identification of high affinity arylpiperazine leads using structure-based drug design. *J Med Chem* **56**: 3446-3455.

Davis IW, Leaver-Fay A, Chen VB, Block JN, Kapral GJ, Wang X, Murray LW, Arendall WB, 3rd, Snoeyink J, Richardson JS, and Richardson DC (2007) MolProbity: all-atom contacts and structure validation for proteins and nucleic acids. *Nucleic Acids Res* **35**: W375-383.

Emsley P, Lohkamp B, Scott WG, and Cowtan K (2010) Features and development of Coot. *Acta Crystallogr D Biol Crystallogr* **66**: 486-501.

Engelhardt S, Grimmer Y, Fan GH, and Lohse MJ (2001) Constitutive activity of the human beta(1)-adrenergic receptor in beta(1)-receptor transgenic mice. *Mol Pharmacol* **60**: 712-717.

Evans P (2006) Scaling and assessment of data quality. *Acta Crystallogr D Biol Crystallogr* **62**: 72-82.

Evans PR (2011) An introduction to data reduction: space-group determination, scaling and intensity statistics. *Acta Crystallogr D Biol Crystallogr* **67**: 282-292.

Lebon G, Warne T, and Tate CG (2012) Agonist-bound structures of G protein-coupled receptors. *Curr Opin Struct Biol* **22**: 482-490.

Leslie AG (2006) The integration of macromolecular diffraction data. *Acta Crystallogr D Biol Crystallogr* **62**: 48-57.

Liapakis G, Ballesteros JA, Papachristou S, Chan WC, Chen X, and Javitch JA (2000) The forgotten serine. A critical role for Ser-2035.42 in ligand binding to and activation of the beta 2-adrenergic receptor. *J Biol Chem* **275**: 37779-37788.

McCoy AJ, Grosse-Kunstleve RW, Adams PD, Winn MD, Storoni LC, and Read RJ (2007) Phaser crystallographic software. *J Appl Crystallogr* **40**: 658-674.

Miller JL and Tate CG (2011) Engineering an ultra-thermostable beta(1)-adrenoceptor. *J Mol Biol* **413**: 628-638.

Miller-Gallacher JL, Nehme R, Warne T, Edwards PC, Schertler GF, Leslie AG, and Tate CG (2014) The 2.1 A resolution structure of cyanopindolol-bound beta1-adrenoceptor identifies an intramembrane Na+ ion that stabilises the ligand-free receptor. *PLoS One* **9**: e92727.

Moukhametzianov R, Warne T, Edwards PC, Serrano-Vega MJ, Leslie AG, Tate CG, and Schertler GF (2011) Two distinct conformations of helix 6 observed in antagonist-bound structures of a beta1-adrenergic receptor. *Proc Natl Acad Sci U S A* **108**: 8228-8232.

Murshudov GN, Skubak P, Lebedev AA, Pannu NS, Steiner RA, Nicholls RA, Winn MD, Long F, and Vagin AA (2011) REFMAC5 for the refinement of macromolecular crystal structures. *Acta Crystallogr D Biol Crystallogr* **67**: 355-367.

Murshudov GN, Vagin AA, and Dodson EJ (1997) Refinement of macromolecular structures by the maximum-likelihood method. *Acta Crystallogr D Biol Crystallogr* **53**: 240-255.

Rasmussen SG, Choi HJ, Fung JJ, Pardon E, Casarosa P, Chae PS, Devree BT, Rosenbaum DM, Thian FS, Kobilka TS, Schnapp A, Konetzki I, Sunahara RK, Gellman SH, Pautsch A, Steyaert J, Weis WI, and Kobilka BK (2011a) Structure of a nanobody-stabilized active state of the beta(2) adrenoceptor. *Nature* **469**: 175-180.

Rasmussen SG, Devree BT, Zou Y, Kruse AC, Chung KY, Kobilka TS, Thian FS, Chae PS, Pardon E, Calinski D, Mathiesen JM, Shah ST, Lyons JA, Caffrey M, Gellman SH, Steyaert J, Skiniotis G, Weis WI, Sunahara RK, and Kobilka BK (2011b) Crystal structure of the beta(2) adrenergic receptor-Gs protein complex. *Nature* **477**: 549-555.

Rosenbaum DM, Cherezov V, Hanson MA, Rasmussen SG, Thian FS, Kobilka TS, Choi HJ, Yao XJ, Weis WI, Stevens RC, and Kobilka BK (2007) GPCR engineering yields high-resolution structural insights into beta2-adrenergic receptor function. *Science* **318**: 1266-1273.

Rosenbaum DM, Zhang C, Lyons JA, Holl R, Aragao D, Arlow DH, Rasmussen SG, Choi HJ, Devree BT, Sunahara RK, Chae PS, Gellman SH, Dror RO, Shaw DE, Weis WI, Caffrey M, Gmeiner P, and Kobilka BK (2011) Structure and function of an irreversible agonist-beta(2) adrenoceptor complex. *Nature* **469**: 236-240.

Roth CB, Hanson MA, and Stevens RC (2008) Stabilization of the human beta2-adrenergic receptor TM4-TM3-TM5 helix interface by mutagenesis of Glu122(3.41), a critical residue in GPCR structure. *J Mol Biol* **376**: 1305-1319.

Schaffner W and Weissmann C (1973) A rapid, sensitive, and specific method for the determination of protein in dilute solution. *Anal Biochem* **56**: 502-514.

Strader CD, Candelore MR, Hill WS, Sigal IS, and Dixon RA (1989) Identification of two serine residues involved in agonist activation of the beta-adrenergic receptor. *J Biol Chem* **264**: 13572-13578.

Venkatakrishnan AJ, Deupi X, Lebon G, Tate CG, Schertler GF, and Babu MM (2013) Molecular signatures of G-protein-coupled receptors. *Nature* **494**: 185-194.

Wacker D, Fenalti G, Brown MA, Katritch V, Abagyan R, Cherezov V, and Stevens RC (2010) Conserved binding mode of human beta2 adrenergic receptor inverse agonists and antagonist revealed by X-ray crystallography. *J Am Chem Soc* **132**: 11443-11445.

Warne T, Chirnside J, and Schertler GF (2003) Expression and purification of truncated, non-glycosylated turkey beta-adrenergic receptors for crystallization. *Biochim Biophys Acta* **1610**: 133-140.

Warne T, Edwards PC, Leslie AG, and Tate CG (2012) Crystal Structures of a Stabilized beta(1)-Adrenoceptor Bound to the Biased Agonists Bucindolol and Carvedilol. *Structure* **20**: 841-849.

Warne T, Moukhametzianov R, Baker JG, Nehme R, Edwards PC, Leslie AG, Schertler GF, and Tate CG (2011) The structural basis for agonist and partial agonist action on a beta(1)-adrenergic receptor. *Nature* **469**: 241-244.

Warne T, Serrano-Vega MJ, Baker JG, Moukhametzianov R, Edwards PC, Henderson R, Leslie AG, Tate CG, and Schertler GF (2008) Structure of a beta1-adrenergic G-protein-coupled receptor. *Nature* **454**: 486-491.

Warne T, Serrano-Vega MJ, Tate CG, and Schertler GF (2009) Development and crystallization of a minimal thermostabilized G protein-coupled receptor. *Protein Expr Purif* **65**: 204-215.

Warne T and Tate CG (2013) The importance of interactions with helix 5 in determining the efficacy of beta-adrenoceptor ligands. *Biochem Soc Trans* **41**: 159-165.

Molecular Pharmacology Fast Forward. Published on September 18, 2015 as DOI: 10.1124/mol.115.101030
This article has not been copyedited and formatted. The final version may differ from this version.



**Footnotes**

This work was funded by a core grant from the Medical Research Council to CGT [MRC U105197215] and AGWL [MRC U105184325], and a Wellcome Trust Clinician Scientist Fellowship awarded to JGB [grant number 073377/Z/03/Z].

Correspondence should be sent to CGT

Financial Disclosure: CGT is a consultant for Heptares Therapeutics Ltd.

Dr C.G. Tate

MRC Laboratory of Molecular Biology,

Francis Crick Avenue,

Cambridge CB2 0QH,

UK

**Figure legends**

Figure 1: Structures of β receptor ligands. (A) noradrenaline; (B) isoprenaline; (C) carazolol; (D) ICI118551; (E) cyanopindolol; (F) 7-methylcyanopindolol. Portions of the structures in blue are regions analogous to those found in noradrenaline. The oxymethylene spacer between the ethanolamine backbone and ligand head group that prevents contraction of the ligand binding pocket in antagonists is shown in red. Noradrenaline and isoprenaline are regarded as full agonists (Baker, 2010a), carazolol and cyanopindolol as weak partial agonists (Baker, 2010a) and ICI18551 as an inverse agonist (Bond et al., 1995; Azzi et al., 2001)

Figure 2: Synthesis of 7-methylcyanopindolol. Reagents and conditions: (a) benzyl bromide, $K_2CO_3$, DMF, 65 ºC, 6 h; (b) (i) Methyl azidoacetate, sodium metal, MeOH, -8 ºC, 3 h, (ii) xylene, 130 ºC, 18 h; (c) (i) 2N NaOH, EtOH, 90 ºC, 4 h, (ii) 3N HCl (aq), rt; (d) (i) $SOCl_2$, $Et_2O$, 0 ºC, 5 h, (ii) $NH_3$, $Et_2O$, -20 ºC, 5 min; (e) $H_2$, 10% Pd/C, MeOH, rt, 8 h; (f) $POCl_3$, 1,4-dioxane, 75 ºC, 15 min; (g) (*S*)-epichlorohydrine, NaOH, 5:2 $H_2O$-1,4-dioxane, rt, 16 h; (h) *tert*-butylamine, 70 ºC, 8 h.

Figure 3: Competition binding curves of ligands to turkey $\beta_1$AR and human $\beta_2$AR. Inhibition of $^3$H-CGP12177 binding to (A) CHO-tβ1 cells and (B) CHO-hβ2 cells was measured in response to cyanopindolol (filled circles), 7-methylcyanopindolol (open circles), carazolol (filled triangles), CGP20712A (open inverted triangles) and ICI118551 (stars). Log $K_D$ values are given in Table I. Bars to the left of the graphs represent total $^3$H-CGP12177 binding (filled bar) and non-specific binding (hatched bar) as determined in the presence of 10 μM propranolol. The concentrations of $^3$H-

CGP12177 present were (A) 0.98 nM and (B) 0.53 nM. Data points are the mean ± s.e.m. of triplicate determinations and these single experiments are representative of (A) 5 and (B) 10 separate experiments.

Figure 4: $^{3}$H-cAMP accumulation in whole cells expressing either turkey $\beta_1$AR or human $\beta_2$AR. The responses to either cyanopindolol (filled circles), 7-methylcyanopindolol (open circles), carazolol (filled triangles) or ICI118551 (stars) was measured either in (A, B) CHO-tβ1 cells or (C, D) CHO-hβ2 cells. Log $EC_{50}$ values are given in Table II and Table III. The inset graph in (A) is a magnified portion of the main graph with the y-axis altered to see only the bottom 2000 dpm. Bars to the left of the graphs represent basal $^{3}$H-cAMP accumulation (filled bar) and the response to 10μM isoprenaline (hatched bar). Data points are the mean ± s.e.m. of triplicate determinations and these single experiments are representative of 4 separate experiments in each case.

Figure 5: CRE-SPAP production in response to 7-methylcyanopindolol and cyanopindolol. (A) CHO-tβ1 cells, (B) CHO-hβ2 cells and (C) CHO-CRE-SPAP cells (parental cells without transfected receptor) were treated with either cyanopindolol (filled circles) or 7-methylcyanopindolol (open circles) and the amount of secreted alkaline phosphatase (SPAP) measured. Log $EC_{50}$ values are given in Table II and Table III. Bars to the left of the graphs represent either basal CRE-SPAP production in the absence of ligand (filled bar) or the response to 10μM isoprenaline (hatched bar). In the parental cell line (C), forskolin was used as the positive control (diagonal hatching of bar). Data points are mean ± s.e.m. of triplicate determinations. These

single experiments are representative of (A) 8, (B) 8 and (C) 4 separate experiments. Error bars are shown, but are smaller than the size of the symbols.

Figure 6: Structure of 7-methylcyanopindolol-bound $\beta_1$AR. (A) Omit map for the ligand binding site. A 2Fo-Fc map was generated where the ligand and the side chains of Ser211 and Ser215 were omitted from the model. The contour level is 1.0 sigma and the figure was produced using CCP4MG. (B, C) Superposition of the structures of $\beta_1$AR bound to 7-methylcyanopindol (receptor in rainbow coloration and the ligand in pink) and cyanopindol (receptor and ligand both grey). The views are either within the membrane plane (A, B) or from the extracellular surface (C), with portions of H3 removed for clarity. The red arrows highlight the different positions of Ser215 in the two $\beta_1$AR structures. The Ballesteros-Weinstein numbers for the residues depicted are as follows: D121, 3.32; S211, 5.42; S215, 5.46; N329, 7.39.

Figure 7: Comparison of the orthosteric binding site of $\beta_1$AR and $\beta_2$AR bound either to carazolol, ICI118551 or 7-methylcyanopindolol. (A) The structure of 7-methylcyanopindolol-bound $\beta_1$AR (rainbow-colored cartoon) was aligned with the structure of carazolol-bound $\beta_1$AR (grey cartoon; PDB code 2YCW) using PyMol (RMSD 0.5 Å, 1734 atoms). A stick format is used to depict the ligands and side chains (labeled) that interact with ligands via hydrogen bonds (7-methylcyanopindolol-bound $\beta_1$AR, carbon atoms in green and hydrogen bonds depicted as red dashed lines; carazolol-bound $\beta_1$AR, carbon atoms in grey and hydrogen bonds as blue dashed lines). (B) The structure of ICI118551-bound $\beta_2$AR (green-colored cartoon; PDB code 3NY8) was aligned with the structure of carazolol-bound $\beta_2$AR (brown cartoon; PDB code 2RH1) using PyMol (RMSD 0.4 Å, 1810

atoms). A stick format is used to depict the ligands and side chains (labeled) that interact with ligands via hydrogen bonds (ICI118551-bound $\beta_2$AR, carbon atoms in green and hydrogen bonds depicted as red dashed lines; carazolol-bound $\beta_2$AR, carbon atoms in grey and hydrogen bonds as blue dashed lines). In both panels, oxygen atoms are red and nitrogen atoms are in blue. The Ballesteros-Weinstein numbers for the residues depicted are as follows ($\beta_1$AR and $\beta_2$AR residues are given respectively): D121 & D113, 3.32; S211 & S203, 5.42; S215 & S207, 5.46; N329 & N312, 7.39; Y333 and Y316, 7.43.

Molecular Pharmacology Fast Forward. Published on September 18, 2015 as DOI: 10.1124/mol.115.101030
This article has not been copyedited and formatted. The final version may differ from this version.



**Table I:** Log $K_D$ values obtained from $^3$H-CGP12177 whole cell binding in CHO-tβ1 and CHO-hβ2 cells. Values represent mean ± s.e.m. of n separate experiments.

| | $\beta_1$AR | | $\beta_2$AR | |
|---|---|---|---|---|
| Ligand | Log $K_D$ | n | Log $K_D$ | n |
| Cyanopindolol | -10.46 ± 0.04 | 6 | -10.49 ± 0.01 | 12 |
| 7-Methylcyanopindolol | -10.37 ± 0.03 | 6 | -10.42 ± 0.04 | 14 |
| Carazolol | -10.23 ± 0.04 | 5 | -10.54 ± 0.04 | 10 |
| (±)-Isoprenaline | -7.34 ± 0.11 | 5 | -6.57 ± 0.08 | 8 |
| ICI118551 | -7.17 ± 0.06 | 5 | -9.36 ± 0.07 | 10 |
| CGP20712A | -7.76 ± 0.05 | 5 | -5.76 ± 0.02 | 10 |

Molecular Pharmacology Fast Forward. Published on September 18, 2015 as DOI: 10.1124/mol.115.101030
This article has not been copyedited and formatted. The final version may differ from this version.



**Table II:** CRE-SPAP gene transcription response and $^{3}$H-cAMP accumulation in ligand-stimulated t$\beta_1$AR-CHO cell lines. Cyanopindolol and carazolol stimulated concentration responses that were best described by a two-component curve. Here the log $EC_{50}$ values are given for each component, the percentage of the response represented by the first component and the percentage of the total response in relation to the isoprenaline stimulation are given. Values represent mean ± s.e.m. of n separate experiments.

| $^{3}$H-cAMP accumulation | | | | | |
|---|---|---|---|---|---|
| | Log $EC_{50}$1 | Log $EC_{50}$2 | % site 1 | % iso max | n |
| Cyanopindolol | -10.25 ± 0.02 | -7.31 ± 0.09 | 64.8 ± 2.4 | 31.8 ± 1.1 | 4 |
| 7-Methylcyanopindolol | -9.76 ± 0.14 | | | 2.3 ± 0.3 | 4 |
| Carazolol | -9.95 ± 0.10 | -6.76 ± 0.06 | 40.2 ± 1.2 | 22.4 ± 0.9 | 4 |
| ICI 118551 | No response | | | | 4 |
| | | | | | |
| CRE-SPAP production | | | | | |
| | Log $EC_{50}$1 | Log $EC_{50}$2 | % site 1 | % iso max | n |
| Cyanopindolol | -10.22 ± 0.06 | -7.19 ± 0.22 | 56.1 ± 5.2 | 40.2 ± 2.4 | 8 |
| 7-methylcyanopindolol | No response | | | | 8 |
| Carazolol | -9.74 ± 0.22 | -6.66 ± 0.25 | 28.7 ± 3.2 | 31.8 ± 3.2 | 4 |

Molecular Pharmacology Fast Forward. Published on September 18, 2015 as DOI: 10.1124/mol.115.101030
This article has not been copyedited and formatted. The final version may differ from this version.



**Table III:** CRE-SPAP and $^{3}$H-cAMP accumulation assays for $\beta_2$AR-CHO cell lines. Log $EC_{50}$ values and % isoprenaline maximal responses obtained from $^{3}$H-cAMP accumulation and CRE-SPAP gene transcription responses in CHO-hβ2 cells. 7-methylcyanopindolol and ICI118551 stimulated inverse agonist concentration responses and thus $IC_{50}$ values are given with a comparison to the response in relation to the basal activity, where basal activity = 100%. Values represent mean ± s.e.m. of n separate experiments.

| $^{3}$H-cAMP accumulation | | | | |
|---|---|---|---|---|
| | Log $EC_{50}$/$IC_{50}$ | % iso max | % basal | n |
| Cyanopindolol | -9.86 ± 0.04 | 8.0 ± 0.9 | - | 8 |
| 7-Methylcyanopindolol | -9.99 ± 0.10 | | 74.5 ± 9.2 | 8 |
| Carazolol | -10.14 ± 0.09 | 1.3 ± 0.2 | - | 8 |
| ICI 118551 | -9.48 ± 0.17 | | 45.3 ± 3.3 | 7 |
| | | | | |
| CRE-SPAP production | | | | |
| | Log $EC_{50}$ | % iso max | % basal | n |
| Cyanopindolol | -9.97 ± 0.05 | 50.8 ± 3.7 | - | 8 |
| 7-Methylcyanopindolol | No response | - | - | 8 |
| Carazolol | -10.30 ± 0.13 | 6.0 ± 1.4 | - | 4 |
| ICI 118551 | No response | - | - | 6 |

**Table IV:** Data collection and refinement statistics

| | $\beta_1$AR-7-methyl-cyanopindolol |
|---|---|
| Number of crystals | 4 |
| Space group | $P2_122_1$ |
| Unit cell parameters<br>a, b, c (Å)<br>α, β, γ (°) | <br>53.0, 61.8, 95.5<br>90, 90, 90 |
| **Data Processing** | |
| Resolution (Å) | 37.8 – 2.4 |
| Rmerge[1] | 0.161 (0.704) |
| $\langle I/\sigma(I)\rangle$ [1] | 8.2 (1.9) |
| Completeness (%)[1] | 98.4 (98.3) |
| Multiplicity[1] | 4.8 (4.9) |
| Wilson B factor (Å$^2$) | 27.7 |
| **Refinement** | |
| Total number of reflections | 11942 |
| Total number of atoms | 2436 |
| Number of waters | 26 |
| Number of lipid molecules | 5 |
| Number of sodium ions | 2 |
| $R_{work}$[2,4] | 0.217 (0.294) |
| $R_{free}$[3,4] | 0.248 (0.285) |
| r.m.s. deviation bonds (Å) | 0.007 |
| r.m.s. deviation angles (°) | 1.29 |

Molecular Pharmacology Fast Forward. Published on September 18, 2015 as DOI: 10.1124/mol.115.101030
This article has not been copyedited and formatted. The final version may differ from this version.



| | |
|---|---|
| Mean atomic B factor (Å$^2$) | 39.35 |
| Estimated coordinate error (Å) | 0.223 |
| Ramachandran plot favoured (%)[5] | 98.94 |
| Ramachandran plot outliers (%)[5] | 0 |

Footnotes.

[1] Values in parentheses are for the highest resolution bin (2.53-2.4 Å)

[2] Number of reflections used to calculate $R_{work}$ : 11942

[3] Number of reflections from a randomly selected subset used to calculate $R_{free}$ :602

[4] Values in parentheses are for the highest resolution bin for refinement (2.46-2.4 Å)

[5] Figures obtained using MolProbity.

Molecular Pharmacology Fast Forward. Published on September 18, 2015 as DOI: 10.1124/mol.115.101030
This article has not been copyedited and formatted. The final version may differ from this version.

Figure 1

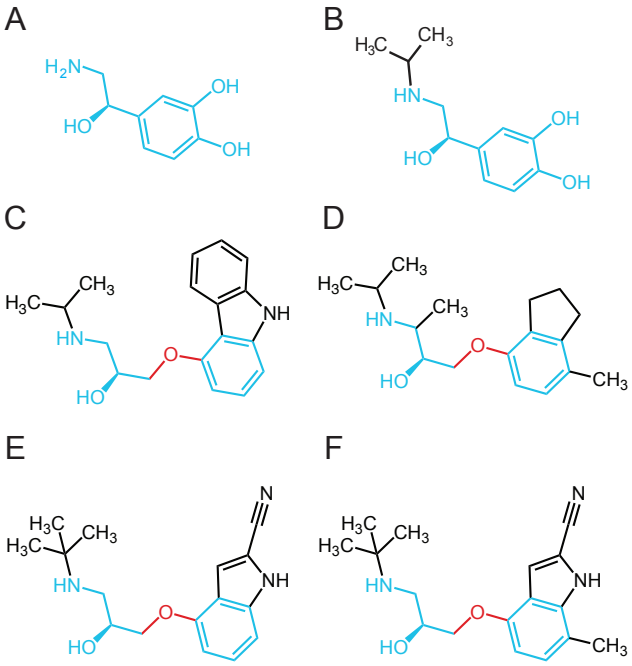

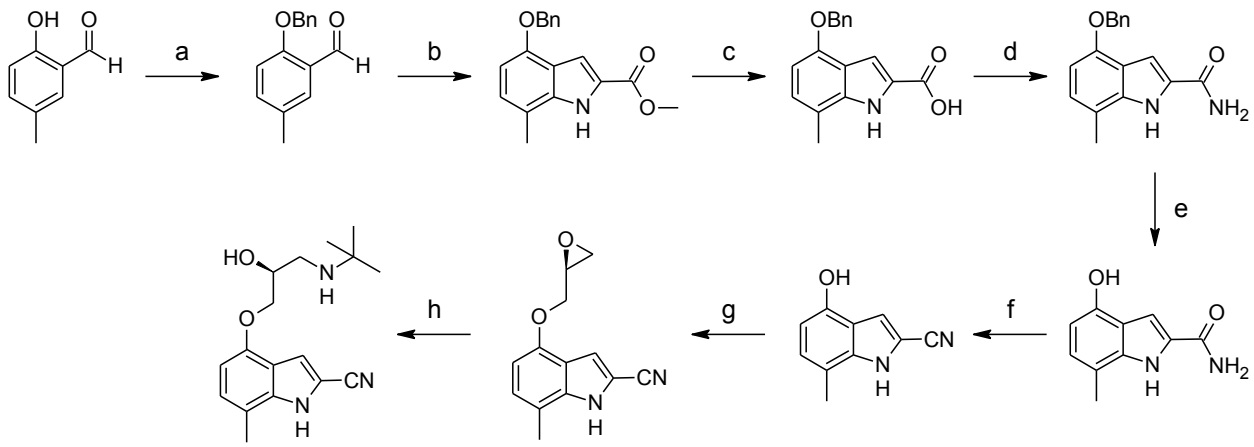

Molecular Pharmacology Fast Forward. Published on September 18, 2015 as DOI: 10.1124/mol.115.101030
This article has not been copyedited and formatted. The final version may differ from this version.

Figure 3

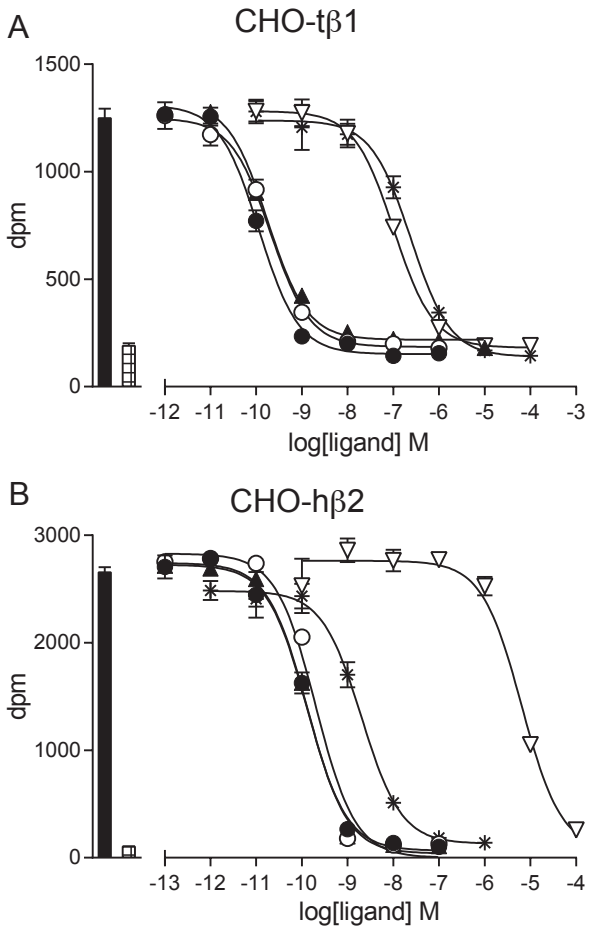

Molecular Pharmacology Fast Forward. Published on September 18, 2015 as DOI: 10.1124/mol.115.101030
This article has not been copyedited and formatted. The final version may differ from this version.

Figure 4

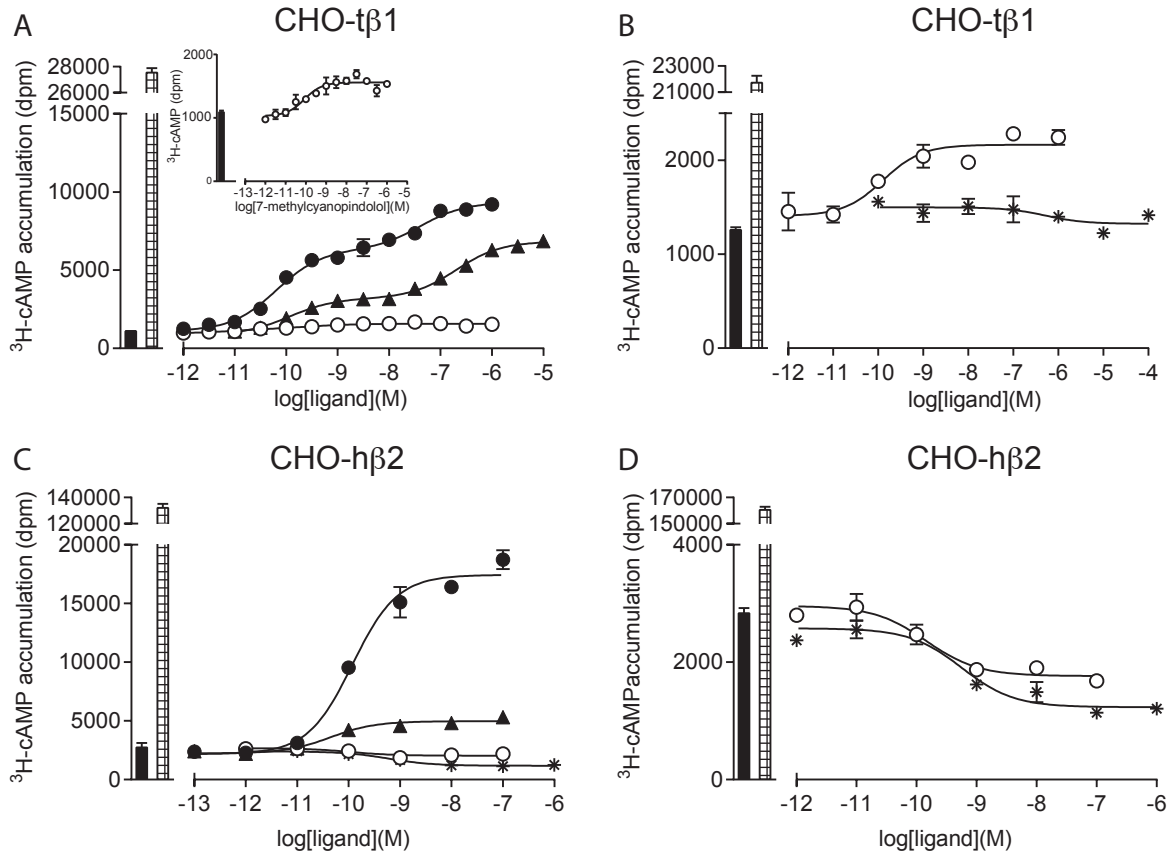

Molecular Pharmacology Fast Forward. Published on September 18, 2015 as DOI: 10.1124/mol.115.101030
This article has not been copyedited and formatted. The final version may differ from this version.

Figure 5

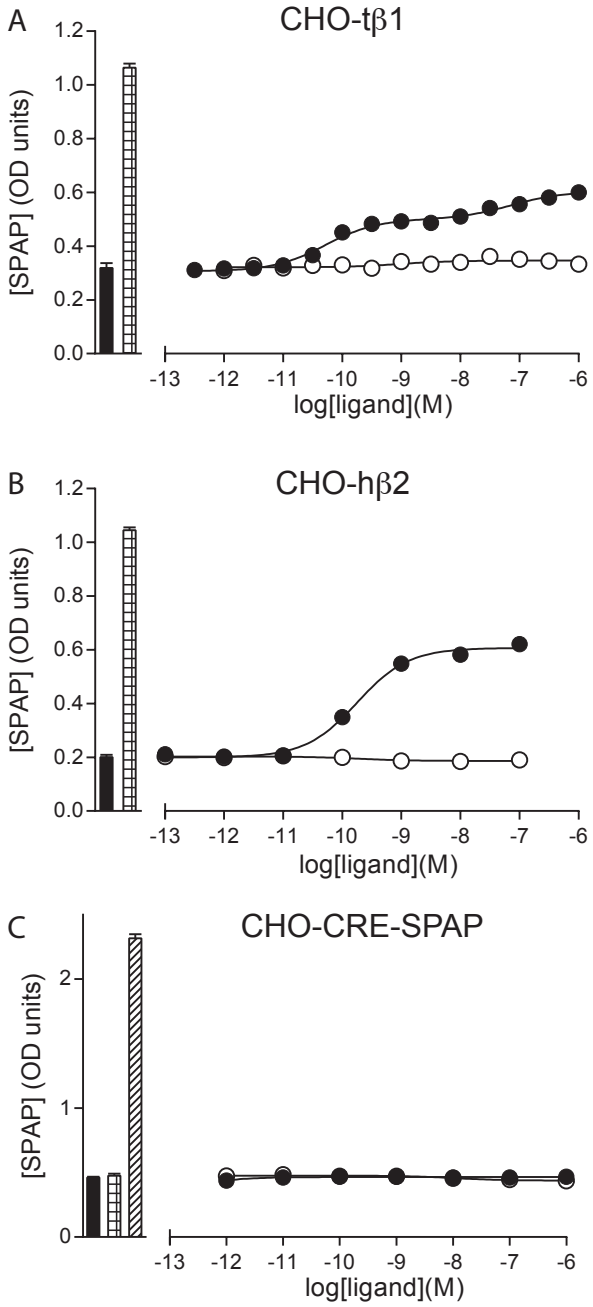

Molecular Pharmacology Fast Forward. Published on September 18, 2015 as DOI: 10.1124/mol.115.101030
This article has not been copyedited and formatted. The final version may differ from this version.

Figure 6

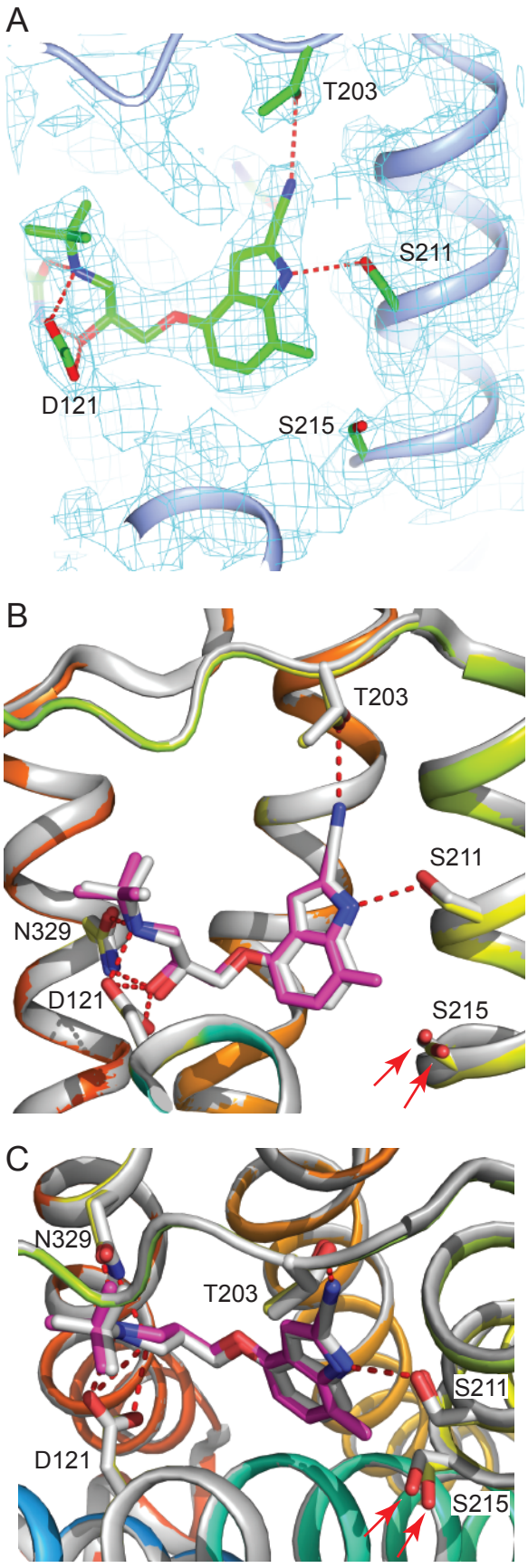

Molecular Pharmacology Fast Forward. Published on September 18, 2015 as DOI: 10.1124/mol.115.101030
This article has not been copyedited and formatted. The final version may differ from this version.

Figure 7